

A Comparative Study of Nanohydroxyapatite Obtained from Natural Shells and Wet Chemical Process

Md. Irfan · P. S. Suprajaa · P. Baraneedharan · B. M. Reddy

Department of Materials Science, Central University of Tamil Nadu, Thiruvarur, 610005, India.

ABSTRACT

In this study, a simple, economic and successful synthesis of nanohydroxyapatite powders was carried out from naturally available bio-waste resources; more specifically crabs shells and eggshells. At first, calcium oxide powders were obtained from crab shells and eggshells via calcination at 800 °C and 1000 °C for 3 hours under ambient air atmosphere. These powders were used as precursor materials for the preparation of the hydroxyapatite samples, which were then compared with the hydroxyapatite obtained from wet chemical process. Structure, morphology and chemical composition of the hydroxyapatite samples were characterized using Fourier transform infrared spectroscopy, Raman spectroscopy, X-ray diffraction, scanning electron microscopy, Energy dispersive X-ray spectroscopy, transmission electron microscopy and selected area electron diffraction. Presence of good quality crystals of hydroxyapatite was confirmed and the measured average size of the hydroxyapatite prepared from crab shells, eggshells and wet chemical process were 293 nm, 182 nm and 106 nm respectively.

© 2020 JMSSE · Indian Thermal Spray Society · Science IN. All rights reserved

ARTICLE HISTORY

Received 20-05-2020

Revised 27-05-2020

Accepted 02-06-2020

Published 10-06-2020

KEYWORDS

Hydroxyapatite

Crab Shells

Eggshells

Calcination

Wet Chemical

Biomaterial

Introduction

Hydroxyapatite (HAp, $\text{Ca}_{10}(\text{PO}_4)_6(\text{OH})_2$) is a major mineral constituent (~70% weight) of human bones and teeth. HAp possesses remarkable properties like biocompatibility, biodegradability, bioactivity and bone-growing/bonding ability [1–4]. HAp has been produced by several methods: sono-chemical, co-precipitation, wet chemical (WC), sol-gel, hydrothermal, ultrasound irradiation, microwave irradiation, electrodeposition, thermal deposition, spray pyrolysis, solid-state reaction and mechanochemical synthesis [4–6]. Alternatively, HAp has been extracted from natural sources like corals, seashells, crab shells, eggshells, fish bones and animal bones [4–12].

Crab shells and eggshells have become attractive sources for the production of HAp, owing to their global availability, low cost, unrestricted supply and due to the development of simple, inexpensive, economical and efficient production methods [6, 10, 13–15]. Dahlan *et al.* produced HAp crystallites (~800 nm) from calcium powders that were obtained after calcination of Merouke Mangrove crab shells [6]. In another study, Chudhuri *et al.* reported the formation of HAp layer on flexible sheet surface of crab shells upon soaking it in dipotassium phosphate (K_2HPO_4) solution [13]. Similarly, Patel *et al.* synthesized HAp from eggshells via reaction between CaO and tricalcium phosphate (TCP) [14]. Gergely *et al.* used attrition milling and ball milling methods to produce HAp from eggshells and phosphoric acid [15]. The authors observed that the attrition milling method yielded nanosize HAp readily, while the ball milling procedure required additional step of calcination at 400 °C for 2 h to obtain HAp. Furthermore, Neelakandeswari *et al.* synthesized HAp from inner membrane of eggshells by using precipitation method [16]. The HAp obtained from the precipitation method has low crystallinity, while compared to the HAp produced from other methods like calcination process. The heat from

calcination enhances the crystallinity of HAp in comparison to the precipitation method.

In this study, Indo-pacific mud or mangrove crab shells (*Scylla serrata*) and eggshells (*Indian country chicken*) were selected as bio-waste resources for synthesis of HAp biomaterial. Additionally, HAp was prepared from precipitation via wet chemical process. Analysis of the HAp samples was done using Fourier transform infrared (FTIR) spectroscopy, Raman spectroscopy, X-ray diffraction (XRD), scanning electron microscopy (SEM), energy dispersive X-ray spectroscopy (EDAX), transmission electron microscopy (TEM) and selected area electron diffraction (SAED).

Experimental

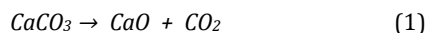
Materials

All chemicals required for the preparation of HAp were of high purity ($\geq 99\%$, analytical grade) and was procured from Sigma-Aldrich, Chennai, India: phosphoric acid (H_3PO_4), dipotassium hydrogen phosphate (K_2HPO_4), calcium nitrate tetrahydrate ($\text{Ca}(\text{NO}_3)_2 \cdot 4\text{H}_2\text{O}$) and diammonium phosphate ($(\text{NH}_4)_2\text{HPO}_4$). Crab shells (*Scylla serrata*) and eggshells (*Indian country chicken*) needed for the present study was collected from southern coastal region of India (Thiruvarur, Tamil Nadu).

Preparation of calcium oxide

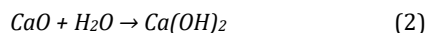
As shown in Figure 1, the calcium oxide needed for synthesis of HAp was obtained by calcination of waste crab shells and eggshells. First, the crab shells and eggshells were carefully washed using deionized (DI) water and then, subjected to drying in an oven at 100 °C for 1 h. Subsequently, these shells were finely grinded using motor and pestle to obtain raw shell powders. Next, the materials were heat treated, using Nabertherm (LHTC 08/16) muffle furnace, at temperatures of 800 °C and 1000 °C for 3 h, at a heating rate of 5 °C/min and under ambient air

atmosphere. The calcination process degrades calcium carbonate into calcium oxide, according to equation (1).

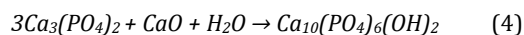
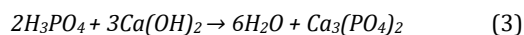


Synthesis of HAp from CaO

HAp was prepared from the CaO powders (CS and ES) by co-precipitation method. A stoichiometric quantity of CaO powder (5 g) were hydrolyzed using 500 mL of DI water, to obtain calcium hydroxide, Ca(OH)_2 solution as follows:



3 mL of phosphoric acid (H_3PO_4) solution was added drop by drop to the Ca(OH)_2 solution at 100°C , under continuous stirring at 800 rpm using a magnetic stirrer. Equations (3) and (4) gives the co-precipitation reactions of tricalcium phosphate (TCP, $\text{Ca}_3(\text{PO}_4)_2$) and hydroxyapatite (HAp, $\text{Ca}_{10}(\text{PO}_4)_6(\text{OH})_2$) respectively.



After 2 h, the milky white solution was cooled to room temperature and the resulting precipitate was filtered, rinsed and dried in an oven at 100°C for 2 h. Then, the HAp (CS and ES) powders were collected and stored in separate vials for further analysis.

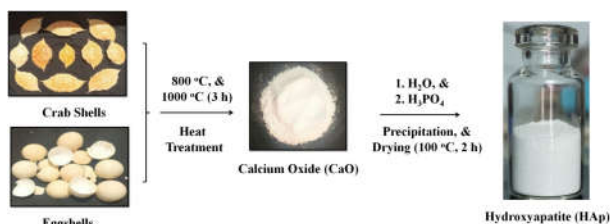
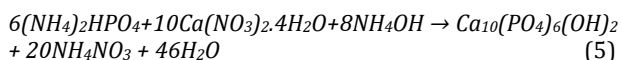


Figure 1: A schematic showing synthesis of HAp from crab shells and eggshells

Synthesis of HAp via wet chemical process

The HAp (CS and ES) powders prepared from the calcination process were compared with the HAp obtained through wet chemical (WC) synthesis. According to equation (5), 0.6 mol of diammonium phosphate ($(\text{NH}_4)_2\text{HPO}_4$), solution was added drop by drop to 1 mol of calcium nitrate tetrahydrate ($\text{Ca}(\text{NO}_3)_2 \cdot 4\text{H}_2\text{O}$) solution and the pH of the reaction mixture was maintained at values < 8 , by the addition of 0.8 mol ammonium hydroxide (NH_4OH) solution.



The above reaction was performed at a constant temperature of $\sim 37^\circ\text{C}$ and under mild stirring for 3 h. This is followed by an additional aging period of 12 h. The precipitate was collected and rinsed thoroughly using DI water to remove any excess ammonia from the reaction mixture. The precipitate was dried at 80°C for duration of 12 h and it was crushed to fine powder using agate mortar and pestle. The white powder of HAp (WC) was stored in a vial for characterization studies.

Characterization of HAp samples

All the three HAp samples (CS, ES and WC) were investigated for structure, morphology and elemental analysis using different instrumental techniques. Molecular spectroscopic studies were done using FTIR (Thermo Nicolet iS50, Thermo Fischer Scientific) Spectrophotometer and Confocal Raman (Witec Alpha 300RA) Microscope. Phase analysis of the samples was carried out using Empyrean (Malvern Panalytical) XRD instrument, consisting of Cu-K α radiation source ($\lambda=1.54 \text{ \AA}$). Morphology and elemental analysis of the HAp samples were performed using Carl Zeiss (MA15/EVO 18) SEM, equipped with Inca 250 EDAX detector. The presence of nanoscale particles in the HAp samples was confirmed using FEI Technai T20 200 KeV TEM, with SAED pattern imaging capability.

Results and Discussion

As described in the experimental section, a simple and economic procedure was considered for the synthesis of HAp (CS, ES and WC) samples. The samples were studied using spectroscopic, diffraction and microscopic techniques.

Spectroscopy

FTIR and Raman spectroscopy was carried out on the HAp (CS, ES and WC) samples to understand the structure and chemical composition (molecular functional groups) of HAp. Figure 2(a) shows the FTIR spectra of HAp (i) CS, (ii) ES and (iii) WC samples. From the FTIR spectra, the presence of functional groups (OH, CO_2 , CO_3 and PO_4) in the samples was confirmed and the FTIR peak values are listed in Table 1. Similarly, the Raman spectra of HAp (i) CS, (ii) ES and (iii) WC samples are shown in Figure 2(b) and the Raman peaks are listed in Table 1. The peak analysis shows the characteristic Raman shifts are due to PO_4^{3-} groups of HAp. Both FTIR and Raman spectra of the HAp samples matches with the reported literature data [17, 18].

Table 1: FTIR and Raman spectrum peak values of HAp functional groups

Spectroscopy	Wave number (cm^{-1})	Functional group
FTIR	562-564	O-P-O bending (ν_4)
	873-889	CO_3^{2-}
	960-1090	Asymmetric stretching, PO_4^{3-} (ν_3)
	1395-1429	CO_3^{2-}
	2850-2980	CO_2
Raman	3157-3652	OH stretching
	420-480	PO_4^{3-} (ν_2 & ν_4), active mode
	570-610	PO_4^{3-} (ν_4), active mode
	940-970	PO_4^{3-} (ν_1), active mode
	1025-1090	PO_4^{3-} (ν_3), active mode

X-ray diffraction

As shown in Figure 3, the XRD spectra of white powders, obtained by calcination of crab shells and eggshells at 800°C and 1000°C for 3 h under ambient air atmosphere, confirms the presence of pure CaO (standard peak data from JCPDS card # 037-1497), with no other additional calcium phases like CaCO_3 and Ca(OH)_2 . From the insets of

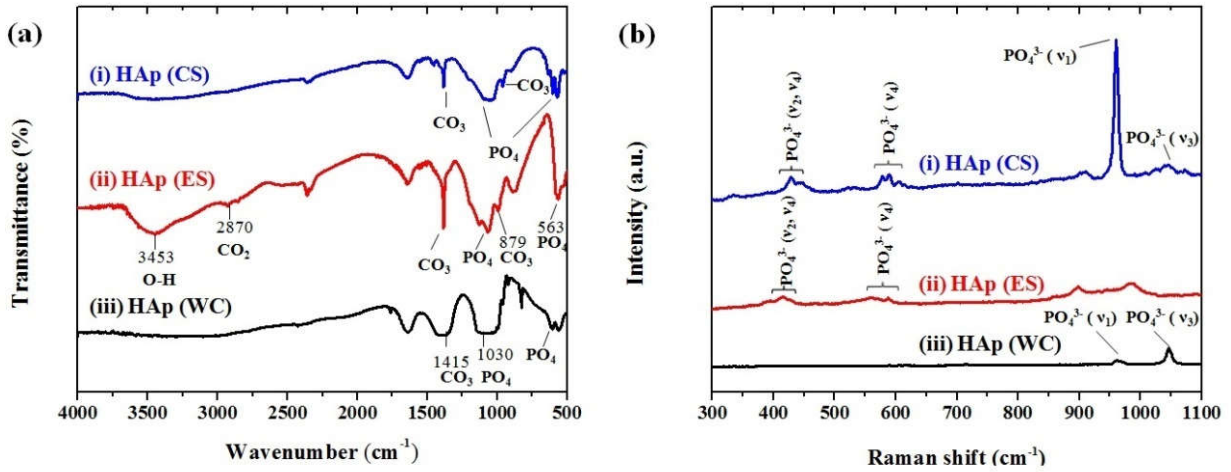


Figure 2: Plots showing (a) FTIR and (b) Raman spectra of hydroxyapatite (HAp) prepared from (i) crab shells, (ii) eggshells and (iii) wet chemical process

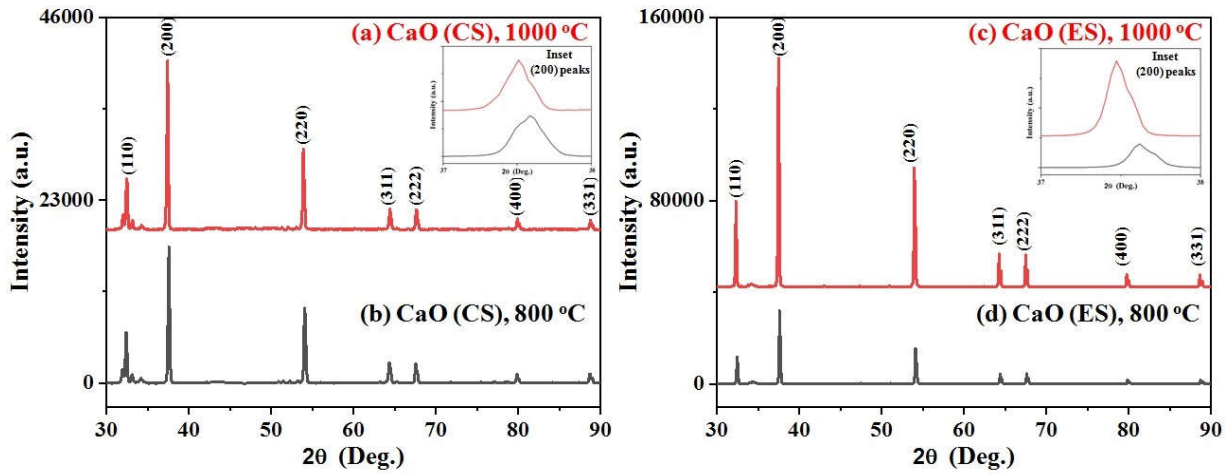


Figure 3: XRD spectra of calcium oxide (CaO) prepared from crab shells (a) at 1000 °C & (b) at 800 °C and eggshells (c) at 1000 °C & (d) at 800 °C with insets of (200) peaks

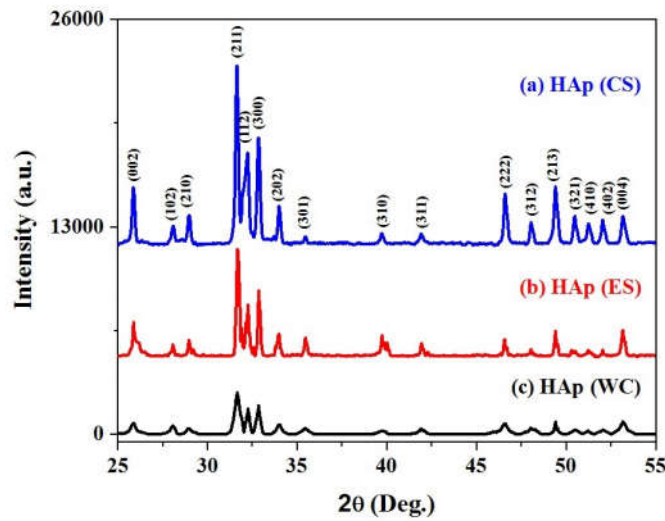


Figure 4: Powder XRD spectra of hydroxyapatite (HAp) prepared using (a) crab shells, (b) eggshells and (c) wet chemical process

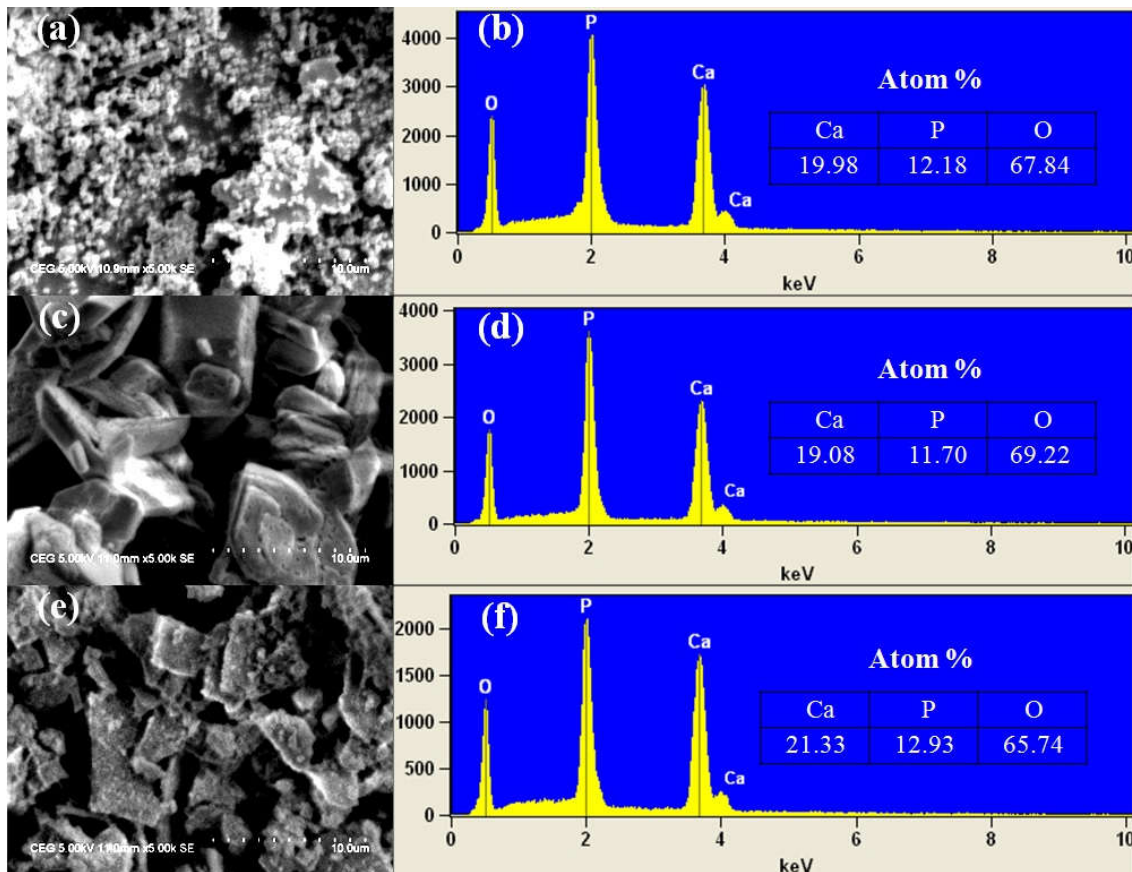


Figure 5: SEM images and corresponding EDAX spectra of HAp samples; (a, b) crab shells, (c, d) eggshells and (e, f) wet chemical process

Figure 3(a) and 3(b), for high intensity reflection (200) at $2\theta \sim 37.5^\circ$, an increase in the sintering temperature from 800°C to 1000°C results in a slight peak shift towards lower diffraction angles. The XRD spectra of HAp (CS and ES) samples obtained from CaO powders, i.e., equation (4) and the XRD spectrum of HAp (WC), i.e., produced from reaction of equation (5) are shown in Figure 4, (a) CS, (b) ES and (c) WC respectively. The peaks were identified, indexed and compared with the standard XRD spectrum of HAp (JCPDS card PDF # 09-0432). The XRD pattern agrees well with the reported literature values for HAp [5]. The sharp and narrow diffraction peaks implies that HAp samples processes fine crystallinity. The lattice constants ($a = b$ and c) for hexagonal crystal lattice structure of the HAp samples was calculated by using Bragg's law and is given by equation (6) as:

$$\frac{1}{d^2} = \frac{4 \times \sin^2(\theta)}{\lambda^2} = \frac{4}{3} \times \left(\frac{h^2 + hk + k^2}{a^2} \right) + \frac{l^2}{c^2} \quad (6)$$

where h , k and l are Miller Indices of Bragg plane, d is spacing between two adjacent (hkl) planes, θ is Bragg's angle and λ is wavelength of monochromatic Cu- $K\alpha$ radiation [1]. The hexagonal unit cell volume 'V' of the HAp samples was determined from equation (7) as [1]:

$$V = 2.589 \times a^2 \times c \quad (7)$$

Table 2 list the lattice constants and cell volume of HAp sample prepared from crab shells, eggshells and wet

chemical method. With the change in the synthesis method, the unit cell dimensions and the cell volume have not altered drastically from the standard International Center for Diffraction Data (ICDD) values, which further confirm that the produced HAp samples are stable [1].

Table 2: Lattice cell constants and cell volume of HAp samples

HAp Sample	Lattice Constant (\AA)		Cell Volume (\AA^3)
	$a (= b)$	c	V
ICDD data	9.4180	6.8840	1580.85
Crab Shells (CS)	9.4535	6.8452	1583.81
Eggshells (ES)	9.4473	6.8443	1581.53
Wet Chemical (WC)	9.4252	6.8438	1574.02

Scanning electron microscopy

The surface morphology of the HAp powders was investigated using SEM and the images are shown in Figure 5, (a) CS, (c) ES and (e) WC. The SEM images of HAp samples reveal the presence of sub-micrometer level agglomerates of HAp crystals. The EDAX analysis was carried out to determine the elemental composition of the HAp samples and the spectra are shown in Figure 5, (b) CS, (d) ES and (f) WC respectively. The EDAX pattern reveals the presence of Ca, P and O elements in the HAp samples, with no other detectable impurities. From the EDAX data, the calculated Ca/P ratios in HAp samples are: (a) CS is 1.64, (c) ES is 1.63 and (e) WC is 1.65. The small change in

Ca/P ratio of synthesized HAp samples, in comparison to the stoichiometric Ca/P ratio (= 1.67) of pure HAp, may be because of loss of Ca^{2+} ions from the HAp unit cell or may be due to substitution of cations such as Na^+ , Mg^{2+} , Al^{3+} in calcium ion vacant sites of HAp unit cell [19, 20]. The possible source of the cations could be from the natural resources because the HAp (CS and ES) in the present study is derived from crab shells and eggshells, while in case of HAp (WC), the cations could be from the chemical reagents (trace metal impurities) that are used during the wet chemical process.

Transmission electron microscopy

Figure 6 shows the TEM images of the HAp (a) CS, (b) ES and WC powders. The average size of the HAp crystals was measured using Nano Measurer 1.2 image analysis tool and the mean size of HAp nanoparticles prepared from crab shells, eggshells and wet chemical process were 293 nm, 182 nm and 106 nm respectively. From Figure 6(d), the SAED pattern of HAp (WC) powder reveals the electron diffraction spots distributed as concentric rings, which further indicates the presence of nanosized crystals. Few reports exist on different methods for producing nanohydroxyapatite from biowaste resources. In this work, we illustrated a simple method for synthesis of nanohydroxyapatite *via* calcination of inexpensive and commonly obtainable bioresources i.e., crab shells and eggshells and from wet chemical process. The results indicate that the produced HAp samples are of good quality, with Ca/P ratio ~ 1.67 and therefore, the produced HAp can be a prospective material for biomedical industry.

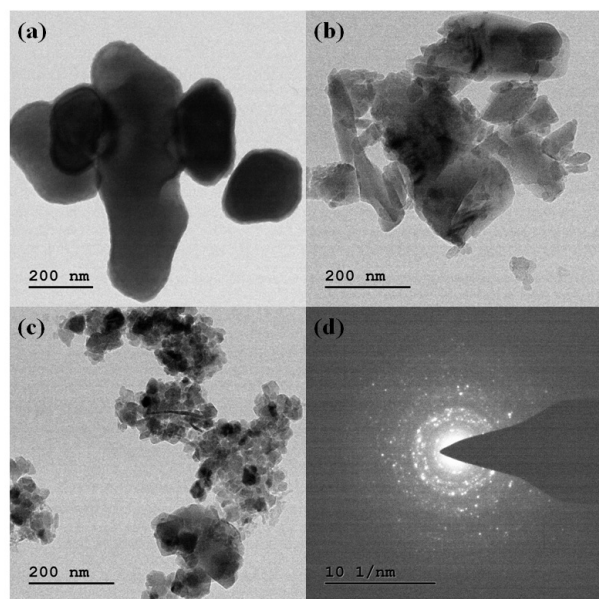


Figure 6: TEM images of hydroxyapatite (HAp) samples from (a) crab shells, (b) eggshells and (c) wet chemical process and (d) corresponding SAED pattern

Conclusions

Nanohydroxyapatite (HAp) powders were synthesized from cheap and widely available bioresources (crab shells and eggshells) *via* a simple calcination, at 800 °C and 1000 °C for 3 h, to produce CaO precursor material and followed by a precipitation process. The produced HAp samples were characterized along with the HAp powder that was

obtained from the wet chemical process. FTIR and Raman spectra of the HAp samples indicate the presence of hydroxyl, carbonate and phosphate functional groups in the molecular structure. XRD analysis of the samples confirms the presence of pure and stable HAp crystallite phases, with no other calcium phases as impurities. The SEM and EDAX studies show that the powders contain sub-micrometer level agglomerates of HAp crystallites, with the Ca/P ratios close to the stoichiometric value of 1.67. From the TEM images, the average size of the HAp crystals was measured to be 293 nm, 182 nm and 106 nm for the samples obtained from crab shells, eggshells and wet chemical process. Therefore, nanoscale hydroxyapatite powders can be efficiently synthesized from crab shells (*Scylla serrata*) and eggshells (*Indian country chicken*) using simple calcination and wet chemical processes for broader range of biomedical applications.

Acknowledgments

The authors would like to thank the Department of Materials Science and the common instrumentation lab facility at Central University of Tamil Nadu (CUTN) for providing access to the necessary instruments during the project period.

References

1. Eslami Hossein, Mohammadreza Tahriri, Fathollah Moztaarzadeh, Rizwan Bader, Lobat Tayebi, Nanostructured Hydroxyapatite for Biomedical Applications: From Powder to Bioceramic, *J. Korean Ceram. Soc.*, 2018, 55 (6), 597-607.
2. O'Hare Peter, Brian J. Meenan, George A. Burke, Greg Byrne, Denis Dowling, John A. Hunt, Biological Responses to Hydroxyapatite Surfaces Deposited via a Co-Incident Microblasting Technique, *Biomaterials*, 2010, 31 (3), 515-522.
3. Hendi A. A, Hydroxyapatite based Nanocomposite Ceramics, *J. Alloy. Comp.*, 2017, 712, 147-151.
4. Sadat-Shojai Mehdi, Mohammad-Taghi Khorasani, Ehsan Dinpanah-Khoshdargi, Ahmad Jamshidi, Synthesis Methods for Nanosized Hydroxyapatite with Diverse Structures, *Acta Biomater.*, 2013, 9 (8), 7591-7621.
5. Sunil B. Ratna, Jagannatham M, Producing Hydroxyapatite from Fish Bones by Heat Treatment, *Mater. Lett.*, 2016, 185, 411-414.
6. Dahlan K., Haryati E, Togibasa O, Characterization of Calcium Powders from Merauke Mangrove Crab Shells, *J. Phys.: Conf. Ser.*, 2019, 1204 (1), 012030.
7. Brzezińska-Miecznik Jadwiga, Krzysztof Haberko, Maciej Sitarz, Mirosław M. Bućko, Beata Macherzyńska. Hydroxyapatite from Animal Bones-Extraction and Properties, *Ceram. Int.*, 2015, 41 (3), 4841-4846.
8. Pu'ad N.A.S. Mohd, Koshy P, Abdullah H. Z, Idris M. I, Lee T. C, Syntheses of Hydroxyapatite from Natural Sources, *Heliyon*, 2019, 5 (5), e01588.
9. Santhosh S, Balasivanandha S. Prabu, Thermal Stability of Nano Hydroxyapatite Synthesized from Sea Shells through Wet Chemical Synthesis, *Mater. Lett.*, 2013, 97, 121-124.
10. Goloshchapov D. L, Kashkarov V. M, Rummyantseva N. A, Seredin P. V, Lenshin A. S, Agapov B. L, Domashevskaya E. P, Synthesis of Nanocrystalline Hydroxyapatite by Precipitation using Hen's Eggshell, *Ceram. Int.*, 2013, 39 (4), 4539-4549.
11. Londoño-Restrepo Sandra M, Cristian F. Ramirez-Gutierrez, Alicia del Real, Efrain Rubio-Rosas, Mario E. Rodriguez-García, Study of Bovine Hydroxyapatite obtained by Calcinations at Low Heating Rates and Cooled in Furnace Air, *J. Mater. Sci.*, 2016, 51 (9), 4431-4441.
12. Janus Anna Maria, Marek Faryna, Krzysztof Haberko, Anna Rakowska, Tomasz Panz, Chemical and Microstructural

- Characterization of Natural Hydroxyapatite derived from Pig Bones, *Microchimica Acta*, 2008, 161 (3-4), 349-353.
13. Chudhuri Biswadeep, Bhadra D, Dash S, Sardar G, Pramanik K, Chaudhuri B. K, Hydroxyapatite and Hydroxyapatite-Chitosan Composite from Crab Shell, *J. Biomimetics Biomater. Tissue Eng.*, 2013, 3 (6), 653-657.
 14. Patel Dinesh K, Min-Hyeok Kim, Ki-Taek Lim, Synthesis and Characterization of Eggshell-Derived Hydroxyapatite Bioceramics. *J. Biosyst. Eng.*, 2019, 44 (2), 128-133.
 15. Gergely Gréta, Ferenc Wéber, Mihály Tóth, Attila Lajos Tóth, Zsolt E. Horváth, Csaba Balázs, Processing of Nano Hydroxyapatite from Eggshell and Seashell, *Mater. Sci. Forum*, 2010, 659, 159-64.
 16. Neelakandeswari N, Sangami G, Dharmaraj N, Preparation and Characterization of Nanostructured Hydroxyapatite using a Biomaterial, *Synth. React. Inorg. Met.-Org. Chem.*, 2011, 41 (5), 513-516.
 17. Prekajski, Marija, Miljana Mirković, Bratislav Todorović, Aleksandar Matković, Milena Marinović-Cincović, Jelena Luković, Branko Matović, Ouzo Effect—New Simple Nanoemulsion Method for Synthesis of Strontium Hydroxyapatite Nanospheres, *J. Eur. Ceram. Soc.*, 2016, 36 (5), 1293-1298.
 18. Zamperini C. A, André R. S, Longo V. M, Mima E. G, Carlos Eduardo Vergani, Ana Lucia Machado, José Arana Varela, Elson Longo, Antifungal Applications of Ag-decorated Hydroxyapatite Nanoparticles, *J. Nanomater.*, 2013, 2013, 174398.
 19. Siddharthan A, Seshadri T. S, Sampath Kumar, Microwave Accelerated Synthesis of Nanosized Calcium Deficient Hydroxyapatite, *J. Mater. Sci: Mater. Med.*, 2004, 15 (12), 1279-1284.
 20. Boskey A. L, *Biomaterials science: An introduction to materials in medicine*, Elsevier Inc. NY, 2013, Ed. 3, 151-161.

